Printed on November 11, 1993

Collective electronic excitations in carbon fullerene clusters

David Tománek

Department of Physics and Astronomy and Center for Fundamental Materials Research

Michigan State University, East Lansing, Michigan 48824-1116

Abstract

Recent theoretical results for the response of C_{20}, C_{60} and C_{70} fullerene clusters to external electromagnetic fields are reviewed. The calculated static response of free C_{60} has large linear and nonlinear components, the latter being much smaller than originally suggested and significantly reduced by screening effects. Random field approximation calculations indicate that the dynamical dipole response of C_{20}, C_{60} and C_{70} is characterized by two strongly collective modes, namely a Mie-type σ-plasmon at $\hbar\omega\approx$20 eV, and a π-plasmon at $\hbar\omega\approx$6 eV. These modes also dominate the response of these systems to multipolar external fields and hence the electron energy loss spectra. The large oscillator strength of these modes is collected from lower-lying particle-hole excitations which consequently experience strong dynamical screening.

Typeset using REVTEX

I. INTRODUCTION

The discovery of the C_{60} "buckyball" molecule [1] and the subsequent synthesis of this and other fullerenes in bulk quantities [2] has triggered an enormous interest in the scientific community in these systems. All fullerenes have a hollow graphitic shell structure composed of three-fold coordinated carbon atoms. The similarity between the large fullerenes and graphite in terms of their local bonding geometry and the sp^2 bonding of carbon atoms suggests that also their dielectric response may be similar. It is not clear, however, whether this similarity can persist down to fullerene sizes of few tens of atoms, where the dielectric response may be dominated by finite size effects, the discreteness of the electronic spectrum, and the large size of the fundamental gap between the highest occupied molecular orbital (HOMO) and the lowest unoccupied molecular orbital (LUMO). In the following, I will review recent calculations of the dielectric response for fullerenes in the range from C_{20} to C_{70}.

In the following Section II, I will summarize the formalism used to determine the response of carbon fullerenes to external electromagnetic fields. In Section III, this formalism will be first used to address the question, whether the semimetallic nature of graphite, with its highly polarizable system of π electrons, is reflected in an unusually large static polarizability of C_{60}. In Section IV, I will discuss results for the dynamical dipole response of free C_{60} molecules, in particular the possibility of exciting collective modes. As will be shown, such collective modes, reminiscent of a Mie plasmon, indeed occur in spite of a large HOMO-LUMO gap of $\approx$2 eV. In Section V, the discussion will be extended to the C_{20} and C_{70} fullerenes and fields of higher multipolarity. Theoretical and experimental results both indicate the occurrence of collective modes in response to external multipolar fields, which can be related to the σ and π plasmon modes occurring in graphite. Interesting consequences of the multipolar response for inelastic electron scattering will be addressed in Section VI. A brief summary and main conclusions will be presented in Section VII.

II. THEORY

The following is a brief summary of the application of linear response theory to determine the response of fullerenes to external fields. This formalism is most appropriate for large systems with mobile electrons, such as the carbon fullerenes, where screening can be significant.

In the independent particle picture, the particle-hole propagator is given by [3]

$$G_0(\mathbf{r},\mathbf{r}';\omega) = \sum_{p,h} \frac{<\mathbf{r}|ph><ph|\mathbf{r}'>}{(\varepsilon_p - \varepsilon_h)^2 - (\hbar\omega + i\eta)^2} \, , \tag{1}$$

where p and h are the particle and hole states, $\varepsilon_{p,h}$ their corresponding energies, $\hbar\omega$ the excitation energy and η its (small) imaginary part. Dynamical screening in the system is described, to first order, by the Random Phase Approximation (RPA) Green function, which is a solution of the integral equation

$$G^{RPA} = G_0 - G_0 V G^{RPA} \, , \tag{2}$$

where $V = e^2/|\mathbf{r} - \mathbf{r}'|$ is the Coulomb interaction among electrons.

Once the RPA Green function is known, the (dynamical) response to any weak external field $F(\mathbf{r})$ is given by

$$S(\omega) = \frac{1}{\pi} \mathrm{Im} < F|G^{RPA}|F> \, . \tag{3}$$

The single-particle spectrum can be conveniently determined using the Linear Combination of Atomic Orbitals (LCAO) Hamiltonian

$$H = \sum_{i,\alpha} \epsilon_i a^\dagger_{i\alpha} a_{i\alpha} + \sum_{i,j,\alpha,\beta} t_{i\alpha,j\beta}(\mathbf{r_{ij}}) a^\dagger_{i\alpha} a_{j\beta} + h.c. \tag{4}$$

Here, i labels the atomic sites and $\alpha = s, p_x, p_y, p_z$ labels the atomic orbitals. ϵ_α is the orbital energy, and $t_{\alpha\beta}$ are the hopping matrix elements between different sites. The single-particle states, used in Eq. (1), are the solutions of the Schödinger equation

$$H|\psi_n> = \varepsilon_n|\psi_n> \, . \tag{5}$$

Here, the single-particle wavefunctions $|\psi_n>$ are linear combinations of s and p orbitals $\varphi_{i\alpha}(\mathbf{r})$ centered on the atoms i, and are given by

$$\psi_n(\mathbf{r}) = \sum_{i,\alpha} c_{i\alpha n}\varphi_{i\alpha}(\mathbf{r}) \; . \tag{6}$$

This expression provides a straight-forward way to evaluate the particle-hole wave functions $<\mathbf{r}|ph>$ used in Eq. (1).

The matrix elements of the Hamiltonian given in Eq. (4) have been determined using the Slater-Koster parametrization [4] in terms of two-center integrals, by performing a careful fit of *ab initio* Local Density Functional (LDA) [5] calculations for C_2, graphite and diamond at different interatomic distances [6]. The diagonal elements of the Hamiltonian are $s-$ and $p-$level energies $\epsilon_s = -7.3$ eV and $\epsilon_p = 0.0$ eV. The off-diagonal matrix elements are a linear combination of Slater-Koster parameters with a d^{-2} distance dependence. Their values for $d = 1.546$ Å, which is the equilibrium nearest-neighbor distance in diamond, are $V_{ss\sigma} = -3.63$ eV, $V_{sp\sigma} = 4.20$ eV, $V_{pp\sigma} = 5.38$ eV, and $V_{pp\pi} = -2.24$ eV.

The electronic spectrum of the C_{60} molecule in equilibrium, obtained using this Hamiltonian, is reproduced in Fig. 1. It is characterized by a relatively large occupied band width $W_{occup} = 19.1$ eV, and a HOMO-LUMO gap of $\Delta E_{\text{HOMO-LUMO}} = 2.2$ eV. These values compare favorably with *ab initio* Local Density Functional results for the bandwidth $W_{occup} = 18.8$ eV [7], $W_{occup} = 19.2$ eV [8], the gap $\Delta E_{\text{HOMO-LUMO}} = 1.8$ eV [7], $\Delta E_{\text{HOMO-LUMO}} = 1.8$ eV [8], and the experimental value $\Delta E_{\text{HOMO-LUMO}} = 1.9$ eV. This formalism has also been used successfully to describe the growth and relative stability of C_n clusters [6]. Most important, this technique is computationally very efficient, which allows the calculation of excitation spectra in molecules as large as tens to hundreds of atoms.

In the following, this formalism will be applied first to address the static response of the C_{60} fullerene to an external electric field.

III. STATIC POLARIZABILITY OF C_{60}

The theoretical work on the static polarizability of C_{60}, published in Ref. [9], has been motivated by a recent experimental report [10] of a very large absolute value [11] of the third-order optical polarizability $|\gamma| = 1.5 \times 10^{-42}$ m^5/V^2 $= 1.07 \times 10^{-28}$ esu for C_{60} molecules in benzene solution. This value would make these systems prime candidates for a direct application in nonlinear optical devices. Subsequent experimental studies [12,13] indicated a substantially smaller value of the hyperpolarizability than the initially observed.

The dipole moment p which is induced by an external electrostatic field $\mathcal{E}$ in an isolated C_{60} molecule is given (to the lowest three orders) by

$$p = \alpha\mathcal{E} + \gamma\mathcal{E}^3 \, . \tag{7}$$

Here, α is the (linear) polarizability and γ is the (third order) hyperpolarizability. This expression takes into account the fact that the second order hyperpolarizability is zero in centrosymmetric systems such as the C_{60} cluster. The polarizabilities can be determined from the energy change of a molecule due to an external field $\mathcal{E}$

$$\Delta E = -\frac{1}{2}\alpha\mathcal{E}^2 - \frac{1}{4}\gamma\mathcal{E}^4 \, . \tag{8}$$

The energy change ΔE in Eq. (8) can be evaluated either directly from

$$\Delta E = E(\mathcal{E}) - E(\mathcal{E} = 0) \tag{9}$$

or by applying perturbation theory to the LCAO Hamiltonian given in Eq. (4). Calculation of α requires a second order, that of γ a fourth order perturbation theory expression, given by

$$\Delta E^{(2)} = 2 \sum_h \sum_p \frac{V_{hp} V_{ph}}{E_h - E_p} \tag{10}$$

and

$$\Delta E^{(4)} = 2\Bigg[\sum_h \sum_p \sum_{p'} \sum_{p''} \frac{V_{hp}V_{pp'}V_{p'p''}V_{p''h}}{(E_h - E_p)(E_h - E_{p'})(E_h - E_{p''})}$$
$$-2\sum_h \sum_p \sum_{p'} \sum_{h''} \frac{V_{hp}V_{pp'}V_{p'h'}V_{h'h}}{(E_h - E_p)(E_h - E_{p'})(E_{h'} - E_{p'})}$$
$$+\sum_h \sum_p \sum_{h'} \sum_{h''} \frac{V_{hp}V_{ph''}V_{h''h'}V_{h'h}}{(E_h - E_p)(E_{h'} - E_p)(E_{h''} - E_p)}$$
$$-\sum_h \sum_p \sum_{p'} \sum_{h'} \frac{V_{hp}V_{ph'}V_{h'p'}V_{p'h}}{(E_h - E_p)(E_h - E_{p'})(E_{h'} - E_p)}\Bigg], \qquad (11)$$

where $V_{ij} = < i| - e\mathcal{E}z|j >$.

This calculation yields a large bare polarizability of the C_{60} molecule $< \alpha_{bare} >=$ 215.0 Å^3, which is one order of magnitude larger than that of other small aromatic molecules such as benzene. When considering the screening of the external field by the induced dipole field in the C_{60}, this value gets reduced to $< \alpha_{screened} >= 35.7$ Å^3. This is only slightly smaller than the value for a classical metal sphere of the same radius R, $< \alpha_{screened} >= R^3 = 42.5$ Å^3, and in the same range as small molecules such as benzene. The right order of magnitude of this value has been confirmed by LDA calculations yielding $< \alpha_{screened} >= 82.7$ Å^3 [14].

The calculated value for the bare third order hyperpolarizability $< \gamma_{bare} >= +346.2 \times 10^{-36}$ esu is larger by more than two orders of magnitude than values found in small aromatic molecules such as benzene. This value also lies well within the range of two of the experiments which find $| < \gamma_{expt} > | = 750 \times 10^{-36}$ esu (Ref. [12]) and $| < \gamma_{expt} > | = 313 \times 10^{-36}$ esu (Ref. [13]), yet well below the value $| < \gamma_{expt} > | = 1.07 \times 10^{-28}$ esu originally reported in Ref. [10]. This apparently good agreement is, however, marred by the intramolecular screening which reduces the molecular hyperpolarizability significantly to $< \gamma_{screened} >= 2.3 \times 10^{-36}$ esu, a value which is no larger than in aromatic molecules such as benzene. It appears as unlikely that this result is a mere artifact of the computational technique, since the LDA calculation of Ref. [14] also finds a very small value of $< \gamma_{screened} >= 7.0 \times 10^{-36}$ esu. While the origin of this discrepancy is presently not resolved, one can suspect the high laser frequency $\hbar\omega \approx 1.2$ eV used in the experiments to be a possible origin of this discrepancy.

In the following, I will review calculations of the dynamical response of fullerenes to

external electromagnetic fields. To illustrate the most important effects, I will start with the dipole response of C_{60}.

IV. DYNAMICAL DIPOLE RESPONSE OF C_{60}

The large static polarizability of C_{60}, discussed in the previous Section, suggests the possibility of a collective response to external dipole fields at least for photon energies $\hbar\omega$ exceeding the HOMO-LUMO gap. The LCAO-RPA calculation of the dynamical dipole response of C_{60}, published in Ref. [15], has been originally motivated by the observed photon absorption strength of C_{60} clusters in solution [16].

As will be shown in the following, the calculated spectrum of Ref. [15] is in quantitative agreement with the experiment in the observed low-frequency region. More important, the RPA calculation also predicted a giant Mie-type resonance at large excitation energies $\hbar\omega \approx$ 20 eV which has subsequently been confirmed by gas phase photoionization experiments [17].

The use of the RPA formalism to describe the response of fullerenes to weak arbitrary fields has been reviewed in Section II. It is useful to note that C_{60} has perfect spherical symmetry, so that good angular quantum numbers can be introduced [15,18]. The total angular momentum $\mathbf{J}$ of a $|ph>$ state, used in Eq. (1), can be written as a sum of an on-ball angular momentum $\mathbf{L}$ and an on-atom angular momentum $\mathbf{l}$, as $\mathbf{J} = \mathbf{L} + \mathbf{l}$. The $\mathbf{L}$ value assigned to a $|ph>$ state depends only on the amplitudes $c_{i\alpha n}$ of the atomic wavefunctions in the $|ph>$ wavefunction, which are defined in Eq. (6). The angular momentum $\mathbf{l}$ describes only the transitions on each site: $l = 0$ results from $s \rightarrow s$ and $p \rightarrow p$; $l = 1$ from $s \rightarrow p$ and $p \rightarrow s$; $l = 2$ from $p \rightarrow p$ transitions [18].

In the particular case of a dynamical dipole field applied to a spherical molecule such as C_{60}, the calculation can be simplified significantly by anticipating the form of the dipole operator which describes the response of the system [6]. The dipole operator D is dominated by two contributions, one from the intersite charge transfer across the molecule, characterized

by $L = 1$ and $l = 0$, and the other from the induced dipole moment on a site, characterized by $L = 0$ and $l = 1$. For a field aligned with the z-axis, D_z can be written as

$$\begin{aligned} D_z &= D_z^{(1)} + D_z^{(2)} \\ &= \sum_{\alpha,i} a^\dagger_{\alpha,i} a_{\alpha,i}\, z(i) + d \sum_i (a^\dagger_{s,i} a_{p_z,i} + a^\dagger_{p_z,i} a_{s,i}) \,, \end{aligned} \tag{12}$$

where $z(i)$ is the z-coordinate of the i-th carbon atom and d is the $s \rightarrow p_z$ dipole matrix element on a carbon atom.

In the independent particle picture, the polarization propagator for the free dipole response is defined in analogy to Eq. (1) as [3]

$$\Pi^{(0)}_{D_z}(\omega) = \sum_{p,h} | < p|D_z|h > |^2 \frac{2(\epsilon_p - \epsilon_h)}{(\epsilon_p - \epsilon_h)^2 - (\omega + i\eta)^2} \,. \tag{13}$$

The full response requires the interaction between electrons, which can be approximated as a pure Coulomb interaction. It is convenient to use a spherical expansion of the potential about the center of the cluster, given by $e^2/|\mathbf{r} - \mathbf{r}'| = e^2 \sum_l r^l_< / r^{l+1}_> P_l(\cos\theta)$. As mentioned above, the response is dominated by the dipole term, for which only the fields generated by $D_z^{(1)}$ and $D_z^{(2)}$ are considered in the following. As I will discuss in the following Section, this approximation reproduces correctly the overall response, but misses out some important details.

The RPA response, as described in Ref. [15], can now be obtained in the following way. In a first simple approximation, one can keep only the charge operator $D_z^{(1)}$, and assume the atomic size to be small in comparison with the hollow "buckyball" radius $R \approx 3.5$ Å, $r_< \approx r_> \approx R$. Then the electron-electron interaction is $e^2\ D_z^{(1)}\ D_z^{(1)}/R^3$. The screened response function Π_1^{RPA} due to $D_z^{(1)}$ in Eq. (12) can be determined using the procedure outlined in Section II. The Dyson equation (2) leads to [3]

$$\Pi_1^{RPA}(\omega) = (1 + \Pi_1^{(0)}(\omega) \frac{e^2}{R^3})^{-1} \Pi_1^{(0)}(\omega) \,. \tag{14}$$

Note that in this approach the Π's are ordinary functions and the equation is algebraic and easily computed. In a more refined approximation, one can consider the dipole moments on the sites, described by $D_z^{(2)}$. The effect will be to replace Eq. (14) by a 2×2 matrix equation

$$\tilde{\Pi} = (\tilde{1} + \tilde{\Pi}^{(0)}\tilde{V})^{-1}\tilde{\Pi}^{(0)} \tag{15}$$

which separates the charge and the internal dipole operators. The elements of the 2×2 free response matrix are

$$\tilde{\Pi}^{(0)}_{nm}(\omega) = \sum_{p,h} < p|D^{(n)}_z|h >< h|D^{(m)}_z|p > \frac{2(\epsilon_p - \epsilon_h)}{(\epsilon_p - \epsilon_h)^2 - (\omega + i\eta)^2} \,. \tag{16}$$

$\tilde{V}$ in Eq. (15) is the 2×2 matrix of the interaction, with the elements $\tilde{V}_{11} = e^2/R^3$, $\tilde{V}_{12} = \tilde{V}_{21} = e^2/2R^3$, and $\tilde{V}_{22} = e^2/2dR^2$.

The lowest optically allowed transitions in C_{60} are found to be $h_u \rightarrow t_{1g}$, $h_g \rightarrow t_{1u}$, and $h_u \rightarrow h_g$, and are shown in Fig. 1(b). The respective excitation energies, obtained using the LCAO Hamiltonian of Eq. (4), are 2.8 eV, 3.1 eV, and 4.3 eV. These values compare favorably with the LDA values 2.9 eV, 3.1 eV and 4.1 eV [7] and are reflected in the free response shown in Fig. 2(a). As will become clear in the following, the electron interaction changes the excitation energies significantly and is essential to obtain even a qualitative understanding of the transition strengths.

The results for the screened response [15], based on the RPA treatment of the LCAO Hamiltonian and the charge dipole operator $D^{(1)}_z$, are reproduced in Fig. 2(b). A comparison with the free response shows that the lowest allowed particle-hole transition is slightly shifted in energy to 2.9 eV and agrees well with the observed [16,19] value of 3.1 eV [see Fig. 2(c)]. The oscillator strength [20] of this transition is drastically reduced by a factor of 400 from the value 3.8 in the free response to 0.010 in the RPA. This brings the transition strength close to the measured [19] oscillator strength of 0.004. The higher excitations shown in Fig. 2(b) are found to be shifted substantially upward in energy as compared to the free response shown in Fig. 2(a). This brings them into fair agreement with the observed [16,19] dipole excitations. These transitions are also screened, but the screening factor is only in the range $10 - 30$. They thus appear relatively strong compared to the low transition, in agreement with the experimental data of Ref. [19].

Since the integrated oscillator strength in the region below 10 eV is substantially below the theoretical upper bound of 240 (based on the *f*-sum rule and ignoring the core electrons),

one expects substantial oscillator strength at higher energies. Fig. 3 displays the excitation spectrum of C_{60} extending up to 40 eV, obtained using several approximations. The $D_z^{(1)}$ free response function, shown in Fig. 3(a), has a broad band of transitions in the "intermediate" energy range $\hbar\omega \approx 10 - 20$ eV. With the electron-electron interaction present, the main effect of the Coulomb field is to collect the strength of these transitions into a single strongly collective excitation. The spectrum shown in Fig. 3(b) has this giant resonance at an unusually high frequency $\hbar\omega \approx 30$ eV. In contrast to the low energy region, the inclusion of the on-site dipole term $D_z^{(2)}$ has a substantial effect on the high-frequency response, as shown in Fig. 3(c). The total integrated oscillator strength is strongly reduced, leaving most of the total strength outside the model space. These extra terms shift the energy of the giant resonance to $\hbar\omega \approx 20$ eV and decrease the oscillator strength by a factor of $\approx$2 when compared to the results in Fig. 3(b). These predictions have been confirmed by the observation of a giant plasmon resonance at these energies in isolated C_{60} clusters [17]. Collective excitations at frequencies ranging between $20 - 30$ eV have also been observed in C_{60} films [21–23].

The high frequency collective mode has its origin in the large valence electron density ρ in the C_{60} cluster, and can be understood qualitatively by considering a conducting spherical shell with a radius $R \approx 3.5$ Å and 240 conduction electrons. Results for the optical transition strength function of this system, based on the program JELLYRPA [24], are shown in Fig. 3(d). The energy of the collective mode agrees with Fig. 3(c), allowing an interpretation of the high frequency collective mode of C_{60} at $\approx$ 20 eV as a Mie plasmon of a conducting shell. It is interesting to note that this frequency is close to the Mie plasmon frequency of a solid metal sphere with 240 free electrons and the radius of the C_{60} cluster, which occurs at $\hbar\omega_{Mie} = \hbar[4\pi\rho e^2/(3m)]^{1/2} \approx$25 eV.

V. DYNAMIC RESPONSE TO MULTIPOLAR FIELDS: C_{20}, C_{60} AND C_{70}

The occurrence of the strongly collective dipole mode in C_{60}, which was discussed in the previous Section, suggests also the existence of collective excitations with higher multipolarities (quadrupolar, octupolar, etc.) in these and other fullerenes. Of particular interest is the frequency dependence of the excitation spectra, the nature of these collective excitations, and the cutoff of collective response for fields with a large multipolarity.

The results presented in the following, which are are based on the LCAO-RPA formalism described in Section II, have been published in Ref. [18]. These calculations consider all parity allowed particle-hole states and are not affected by the restriction to the dominating values for the on-ball angular momentum **L** and the on-atom angular momentum l, namely $(L,l) = (1,0)$ or $(0,1)$, imposed in Ref. [15] and discussed in Section V. Fragmentation of the oscillator strength due to the coupling to more complicated states can not be described by RPA. This coupling of the RPA modes to surface electronic oscillations is addressed by the Landau damping, which can be modeled by an imaginary part in the energy $\eta \propto \hbar\omega$ in Eq. (1), similar to Ref. [25].

The calculated free and RPA response of carbon fullerenes to an external multipolar field $F(\mathbf{r}) = r^L Y_{L,M}(\hat{\mathbf{r}})$, for $L = 0 - 8$ ($F(\mathbf{r}) = r^2$ for $L = 0$), is presented in Fig. 4. Results for the particular fullerenes C_{20}, C_{60}, and C_{70} are given in Fig. 4(a), (b), and (c), respectively. Except for the monopole, all other multipole spectra are characterized by a low-frequency peak at $\hbar\omega \approx 6 - 10$ eV and a high-frequency peak at $\hbar\omega \approx 18 - 22$ eV. These features are nearly independent of size, and are also observed in the elongated C_{100} tubule.

The multipolarity L of the external field is given by the ratio of the circumference of the fullerene and the wavelength of the surface mode, $L = 2\pi R/\lambda = qR$. The maximum expected multipolarity of a collective electronic excitation L_{max} can be estimated by comparing the C-C bond length d_{C-C} to $\lambda/2$, yielding $L_{max} = \pi R/d_{C-C}$. This criterion gives $L_{max} \approx 5$ for C_{20} and a larger value $L_{max} \approx 8$ for C_{60} and C_{70}. This estimate agrees very well with the RPA results in Fig. 4. The states with higher angular momentum are essentially single-particle

in nature and show little collective behaviour.

The low-frequency mode around 6-10 eV and the high-frequency mode around 18-22 eV, which have been also observed in electron energy loss spectroscopy of C_{60} fullerite films [23], are the obvious analogues of the π and σ plasmons in graphite [26]. In graphite the low-frequency π mode has been interpreted by the in-plane response of the weakly bound p_π system to a field parallel to the layers. The high-frequency σ mode has been assigned to the out-of-plane motion of the strongly bound σ system of s and p electrons in response to a field perpendicular to the layers. A simple jellium plate model of a graphite monolayer would show the π plasmon at $\hbar\omega = 0$ and the σ plasmon at a much higher finite frequency.

The high-frequency σ mode, which has been already discussed in Section V (albeit in a more approximate way) agrees quite well with the giant resonance observed in the photoionization spectrum [17]. The slight red-shift by 2-3 eV of the calculated peak with respect to the experiment could be partly due to an insufficiently precise parametrization of the LCAO Hamiltonian underlying this calculation, or the fact that $\hbar\omega_\sigma$ lies very close to $3\hbar\omega_\pi$ opening the possibility of a resonant coupling between these modes. A more precise treatment of the excitation spectrum including multiparticle-hole excitations, which are responsible for the Landau damping, would require a formalism beyond the RPA framework.

VI. INELASTIC ELECTRON SCATTERING OF C_{60} AND C_{70}

Since a plane wave representing a monochromatic electron beam has contributions from all multipoles, one can expect that collective excitations with large multipolarities can be observed in an electron energy loss spectroscopy (EELS) experiment. The theoretical description, given in Ref. [18], is based on the differential cross section for electron excitation in the Born approximation,

$$\begin{aligned}\frac{d^2\sigma}{d\Omega d\omega} &= \left(\frac{e^2 m}{\hbar^2}\right)^2 \frac{4p'}{pq^4} |<\omega| \sum_n \exp(-i\mathbf{q}\cdot\mathbf{r}_n)|0>|^2 \\ &= \left(\frac{e^2 m}{\hbar^2}\right)^2 \frac{4p'}{pq^4} S(\mathbf{q},\omega)\,. \end{aligned} \tag{17}$$

Here, p and p' are the initial and final linear momenta of the electron, m is the mass of the electron, $\mathbf{q} = \mathbf{p} - \mathbf{p}'$ is the momentum transfer, and $\hbar\omega$ is the energy transfer. $S(\mathbf{q},\omega)$ is the spectral function (or dynamical structure factor) of the scattering fullerene which depends solely on the properties of this molecule.

For a fixed value of $\mathbf{q}$, the calculated $S^{RPA}(\mathbf{q},\omega)$ of C_{60} and C_{70}, obtained using the LCAO-RPA formalism [18], is dominated by two peaks. These resonances lie at excitation energies around $6-10$ eV and around $18-22$ eV, and correspond to the π and σ modes discussed in the previous Sections. A similar two-peak spectrum has recently been observed on C_{60} and C_{70} gas targets [27]. The maximum of $S(\mathbf{q},\omega)$ occurs at at momentum transfer values $q \approx 1.5-2$ Å. This suggests that the response is mainly due to multipolar components of the electron plane wave which are characterized by $L \approx qR \approx 5-7$. This is consistent with the strongest occurrence of the π and σ modes in C_{60} and C_{70} for these field multipolarity values L.

VII. SUMMARY AND CONCLUSIONS

In summary, the LCAO-RPA formalism has been found successful in determining the polarizability and electronic excitation spectra of C_{20}, C_{60} and C_{70} fullerene clusters.

The calculated static polarizability of free C_{60} has large linear and nonlinear components, the latter being much smaller than originally suggested and significantly reduced by screening effects. Random field approximation calculations indicate that the dynamical dipole response of isolated C_{20}, C_{60}, and C_{70} is characterized by two strongly collective modes, namely a Mie-type σ-plasmon at $\hbar\omega \approx 20$ eV, and a π-plasmon at $\hbar\omega \approx 6$ eV. These modes also dominate the response of these systems to multipolar external fields with a multipolarity $L \lesssim 8$ and hence shape the electron energy loss spectra. The large oscillator strength of these modes is collected from lower-lying particle-hole excitations which consequently experience strong dynamical screening.

The LCAO-RPA formalism, in spite of its success, has certain limitations. The single-

particle spectrum of the fullerenes, as given by the LCAO Hamiltonian, spans a finite-dimensional model space. Even though such a description seems to account very well for the electronic response of the systems investigated, sum rules are strongly violated [15]. Effects of the exchange and correlation energy on the excitations energies have only approximately been addressed in the LCAO parametrization, and treatment of self-consistency in the excitation spectra is only approximate. Finally, the fragmentation of the collective excitations into multiparticle-hole excitations goes beyond the RPA description and has not been included explicitly. In spite of these limitations, the overall agreement with available experimental data is surprisingly good.

ACKNOWLEDGEMENTS

Most of the results discussed in this review have been obtained in a fruitful collaboration with Prof. George Bertsch and Prof. Aurel Bulgac, as well as our former graduate students Dr. Neng-Jiu Ju and Dr. Yang Wang. This work has been supported by the National Science Foundation under Grant No. PHY-8920927.

REFERENCES

[1] H.W. Kroto, J.R. Heath, S.C. O'Brien, R.F. Curl, and R.E. Smalley, Nature **318**, 162 (1985).

[2] W. Krätschmer, L.D. Lamb, K. Fostiropoulos, and D.R. Huffman, Nature **347**, 354 (1990).

[3] G.D. Mahan, *Many-Particle Physics*, (Plenum Press, New York, 1981).

[4] J.C. Slater and G.F. Koster, Phys. Rev. **94**, 1498 (1954).

[5] P. Hohenberg and W. Kohn, Phys. Rev. **136**, B864 (1964); W. Kohn and L.J. Sham, Phys. Rev. **140**, A1133 (1965).

[6] David Tománek and Michael A. Schluter, Phys. Rev. Lett. **67**, 2331 (1991).

[7] Susumu Saito and Atsushi Oshiyama, Phys. Rev. Lett. **66**, 2637 (1991).

[8] M. Schlüter, M. Lannoo, M. Needels, G.A. Baraff, and D. Tománek, J. Phys. Chem. Solids **53**, 1473 (1992), and (private communication).

[9] Yang Wang, George F. Bertsch and David Tománek, Z. Phys. D **25**, 181 (1993).

[10] W.J. Blau, H.J. Byrne, D.J. Cardin, T.J. Dennis, J.P. Hare, H.W. Kroto, R. Taylor and D.R.M. Walton, Phys. Rev. Lett. **67**, 1423 (1991).

[11] Present experimental methods are unable to determine the sign of γ in C_{60}.

[12] Ying Wang and Lap-Tak Cheng, J. Phys. Chem. **96**, 1530 (1992).

[13] Z.H. Kafafi, J.R. Lindle, R.G.S. Pong, F.J. Bartoli, L.J. Lingg and J. Milliken, Chem. Phys. Lett. **188**, 492 (1992); Z.H. Kafafi, F.J. Bartoli, J.R. Lindle, and R.G.S. Pong, Phys. Rev. Lett. **68**, 2705 (1992).

[14] A.A. Quong and M.R. Pederson, Phys. Rev. BR **46**, 12906 (1992).

[15] G.F. Bertsch, A. Bulgac, D. Tománek and Y. Wang, Phys. Rev. Lett. **67**, 2690 (1991).

[16] H. Ajie, M.M. Alvarez, S.J. Anz, R.D. Beck, F. Diederich, K. Fostiropoulos, D. R. Huffman, W. Kratschmer, Y. Rubin, K.E. Schriver, D. Sensharma, and R.L. Whetten, J. Phys. Chem. **94**, 8630 (1990).

[17] I.V. Hertel, H. Steger, J. de Vries, B. Weisser, C. Menzel, B. Kamke and W. Kamke, Phys. Rev. Lett. **68**, 784 (1992).

[18] A. Bulgac and N. Ju, Phys. Rev. B **46**, 4297 (1992); Nengjiu Ju, Aurel Bulgac and John W. Keller, Phys. Rev. B **48**, 9071 (1993).

[19] J.R. Heath, R.F. Curl, and R.E. Smalley, J. Chem. Phys. **87**, 4236 (1987).

[20] The oscillator strength is defined by $f = 2m| < f|D_z|i > |^2(E_f - E_i)/\hbar^2$.

[21] J.H. Weaver, J.L. Martins, T. Komeda, Y. Chen, T.R. Ohno, G.H. Kroll, N. Troullier, R.E. Haufler and R.E. Smalley, Phys. Rev. Lett. **66**, 1741 (1991).

[22] Yahachi Saito, Hisanori Shinohara, and Akinori Ohshita, Jpn. J. Appl. Phys. **30**, L1068 (1991).

[23] G. Gensterblum, J.J. Pireaux, P. Thiry, R. Caudano, J.P. Vigneron, P. Lambin and A.A. Lucas, Phys. Rev. Lett. **67**, 2171 (1991).

[24] G.F. Bertsch, Computer Physics Comm. **60**, 247 (1990).

[25] H. Esbensen and G.F. Bertsch, Phys. Rev. Lett. **25**, 2257 (1984).

[26] K. Zeppenfeld, Z. Phys. **211**, 391 (1968); K. Zeppenfeld, Z. Phys. **243**, 229 (1971); H.H. Venghaus, Phys. Stat. Sol. (b) **71**, 609 (1975); R. Klucker, M. Skibowski and W. Steinmann, *ibid*, **65**, 703 (1974); U. Büchner, *ibid*, **81**, 227 (1977); U. Diebold, A. Preisinger, P. Schattsdchneider and P. Varga, Surf. Sci. **197**, 430 (1988).

[27] J.W. Keller and M.A. Coplan, Chem. Phys. Lett. **193**, 89 (1992).

FIGURES

FIG. 1. (a) Single-particle energy level spectrum of a C_{60} cluster, obtained using the LCAO Hamiltonian defined in Eq. (4) and described in Ref. [6]. (b) Detailed view of the energy level spectrum in the vicinity of the Fermi level, with optically allowed transitions indicated by arrows. The levels have been sorted by symmetry (from Ref. [15], ©American Physical Society 1991).

FIG. 2. (a) Free response and (b) RPA response of C_{60} clusters to an external time-dependent dipole field (solid line). The sharp levels have been broadened by adding an imaginary part $\eta = 0.2$ eV to the energy. The dashed line indicates the integrated oscillator strength. (c) Observed photoabsorption spectrum of Ref. [16] (from Ref. [15], ©American Physical Society 1991).

FIG. 3. Dipole response of C_{60} clusters to an external electromagnetic field, shown in an expanded energy region. (a) Free response, (b) RPA response based on the charge term $D_z^{(1)}$, and (c) RPA response based on both the charge and the dipole terms $D_z^{(1)}$ and $D_z^{(2)}$ in Eq. (12). (d) RPA response of a thin jellium shell, describing the electron-electron interactions in LDA. The response functions are given by the solid line, and the integrated oscillator strengths are shown by the dashed lines (from Ref. [15], ©American Physical Society 1991).

FIG. 4. Free (dotted lines) and RPA (solid lines) response of (a) C_{20}, (b) C_{60}, and (c) C_{70} to external multipolar fields $F(\mathbf{r}) = r^L Y_{L,M}(\hat{\mathbf{r}})$, for $L = 0 - 8$ ($F(\mathbf{r}) = r^2$ for $L = 0$). Damping of the sharp excitations has been described by an imaginary part of the energy $\eta = \hbar\omega/8$ in Eq. (1). (from Ref. [18], ©American Physical Society 1993).

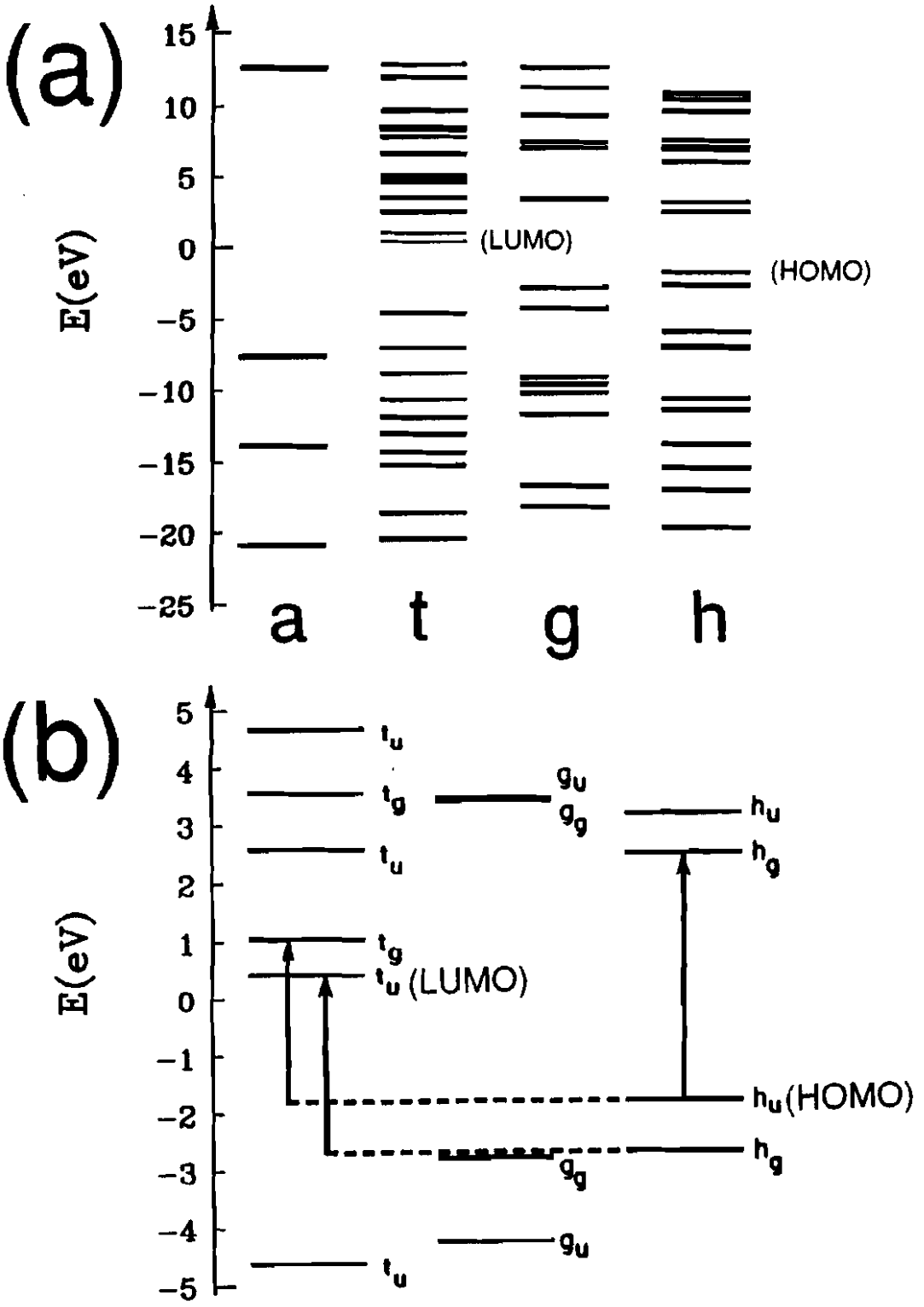
(a)
E(eV)
15
10
5
0
−5
−10
−15
−20
−25
(LUMO)
(HOMO)
a
t
g
h
(b)
E(eV)
5
4
3
2
1
0
−1
−2
−3
−4
−5
t_u
t_g
t_u
t_g
t_u (LUMO)
t_u
g_u
g_g
g_g
g_u
h_u
h_g
h_u (HOMO)
h_g

Figure 1

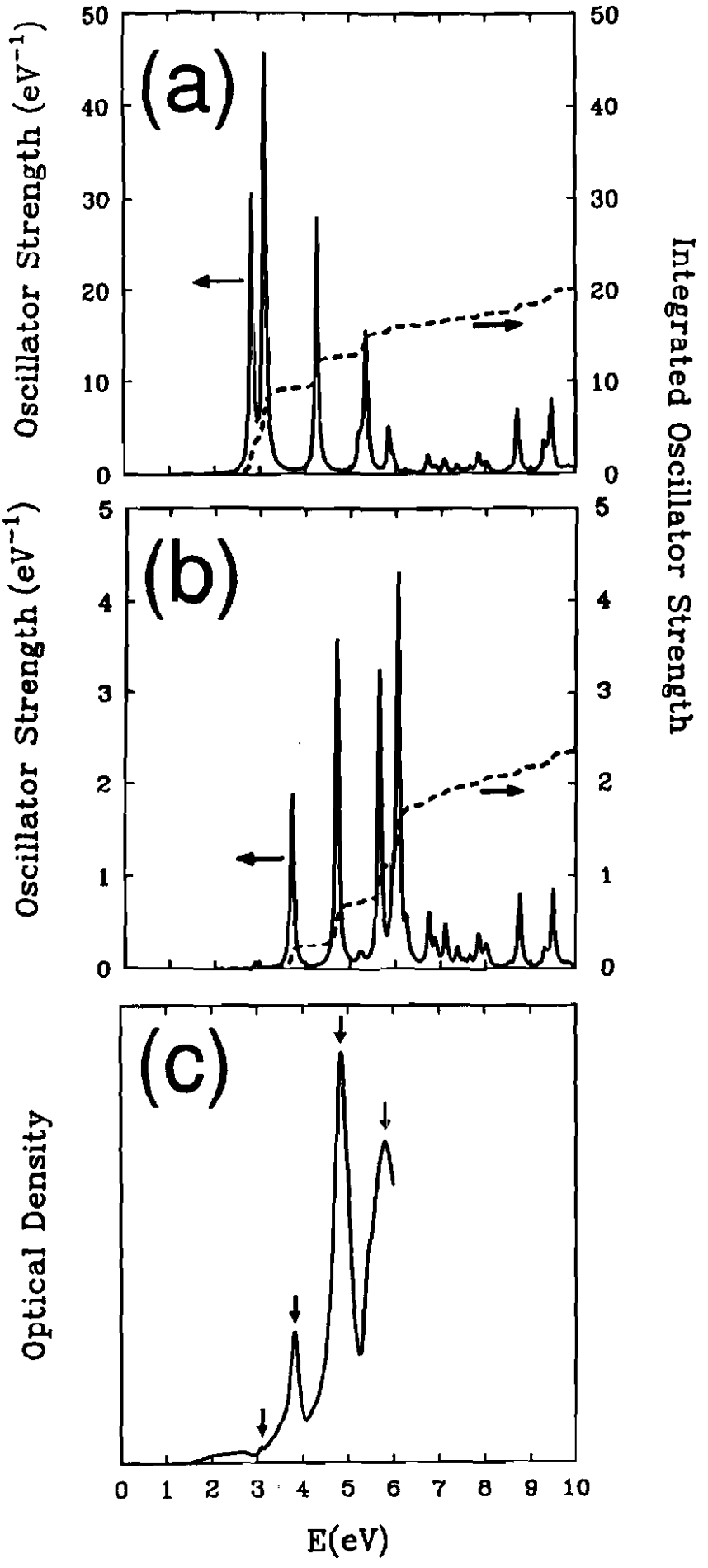
(a)
(b)
(c)
Oscillator Strength (eV^{-1})
Integrated Oscillator Strength
Optical Density
E(eV)
0
10
20
30
40
50
1
2
3
4
5
6
7
8
9

Figure 2

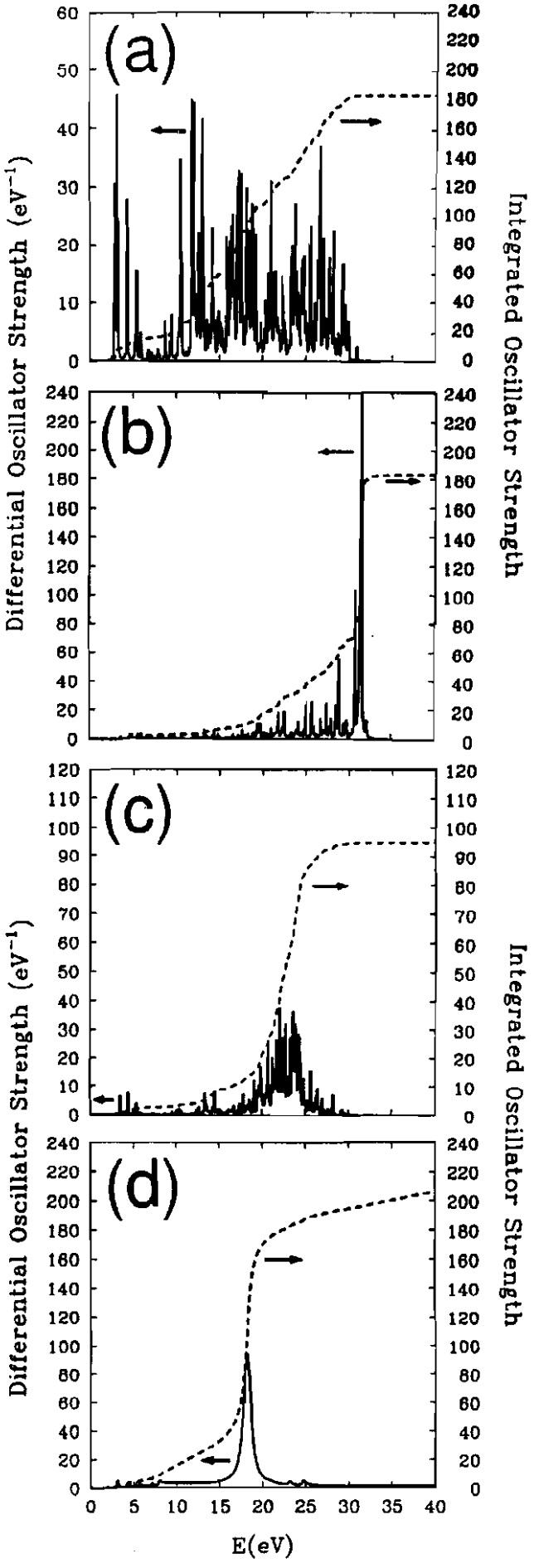
(a)
(b)
(c)
(d)
Differential Oscillator Strength (eV^{-1})
Integrated Oscillator Strength
E(eV)

Figure 3

(a)

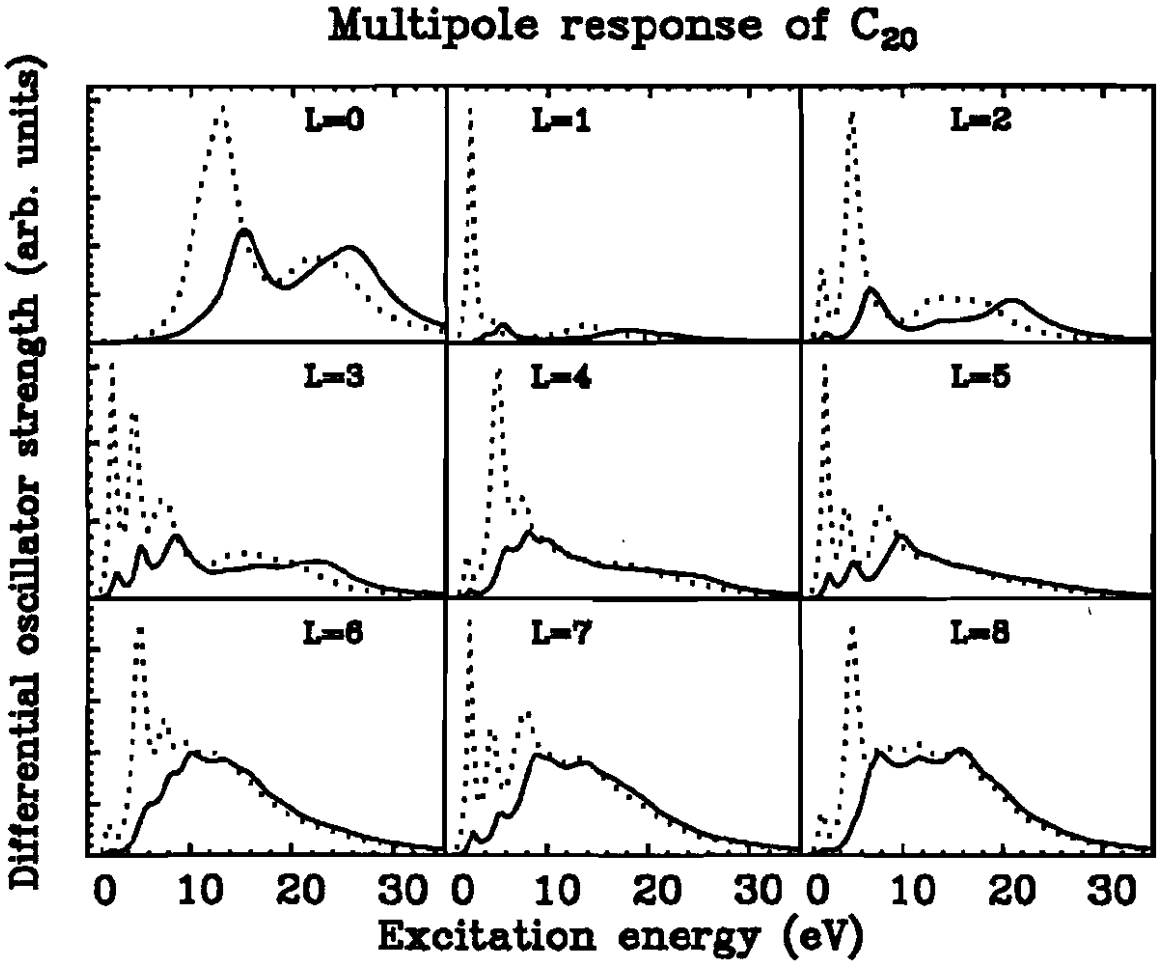
Multipole response of C_{20}
Differential oscillator strength (arb. units)
L=0
L=1
L=2
L=3
L=4
L=5
L=6
L=7
L=8
0
10
20
30
Excitation energy (eV)

Figure 4(a)

(b)

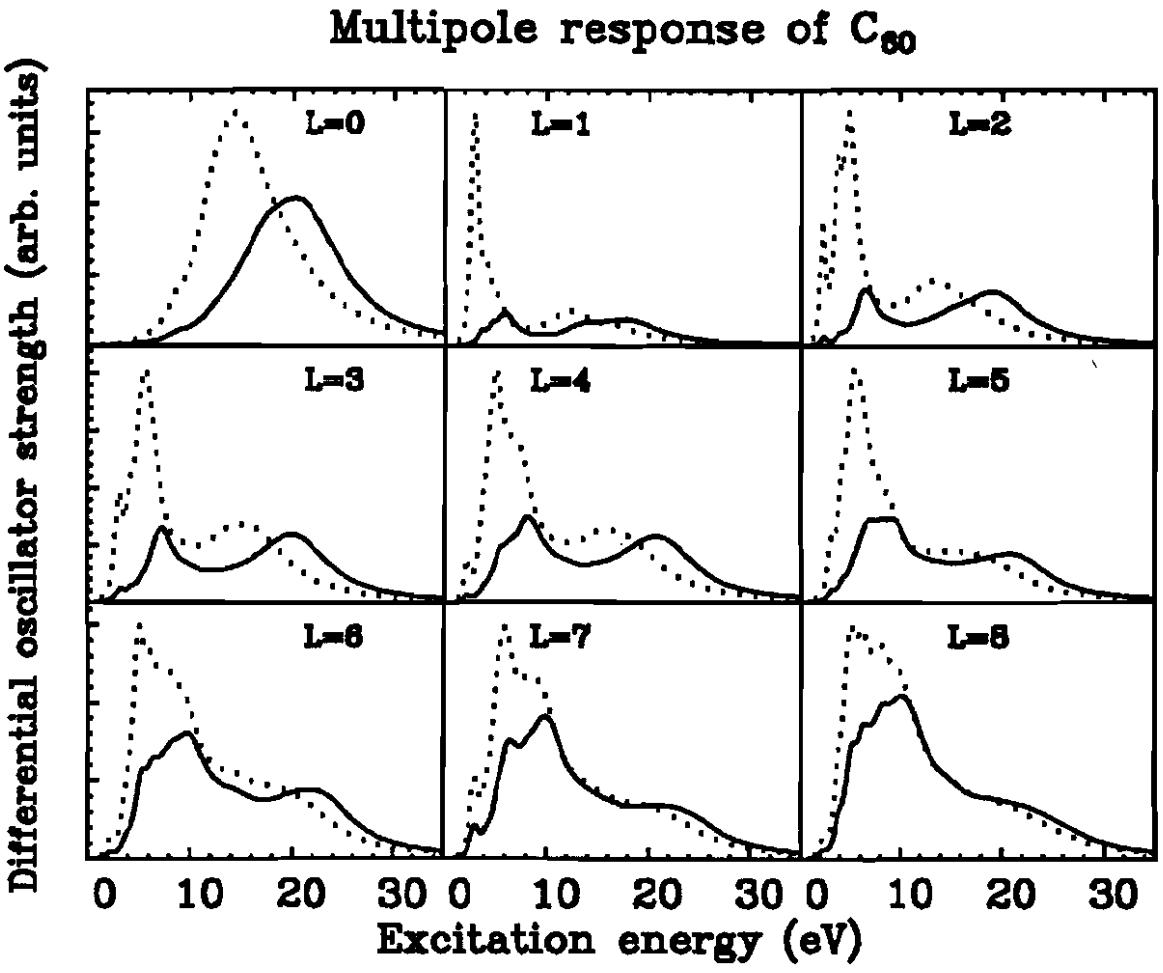
Multipole response of C_{60}
L=0
L=1
L=2
L=3
L=4
L=5
L=6
L=7
L=8
Differential oscillator strength (arb. units)
0
10
20
30
Excitation energy (eV)

Figure 4(b)

(C)

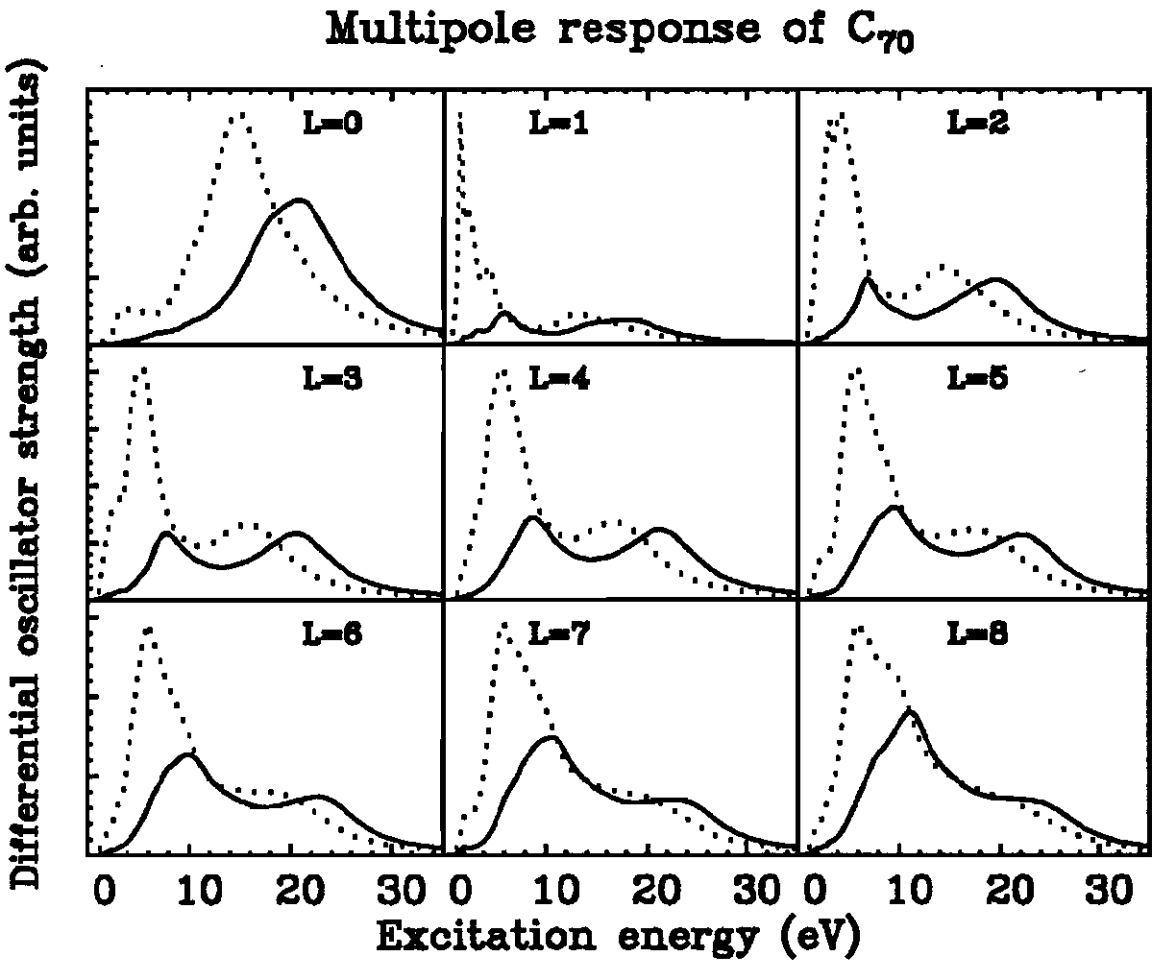
Multipole response of C_{70}
L=0
L=1
L=2
L=3
L=4
L=5
L=6
L=7
L=8
Differential oscillator strength (arb. units)
0
10
20
30
Excitation energy (eV)

Figure 4(c)